Qi *et al. Radiation Oncology* (2025) 20:48
https://doi.org/10.1186/s13014-025-02621-y

Radiation Oncology

RESEARCH Open Access

Gantry-based pencil beam scanning proton therapy for uveal melanoma: IMPT versus proton arc therapy

Hang Qi[1], Lei Hu[2], Sheng Huang[3], Yen-Po Lee[4], Francis Yu[1], Qing Chen[1], Yunjie Yang[5], Minglei Kang[1], Huifang Zhai[1], Milo Vermeulen[1], Andy Shim[1], Peter Park[1], Xuanfeng Ding[6], Jun Zhou[7], David H. Abramson[5], Jasmine H. Francis[5], Charles B. Simone 2nd[1,5], Christopher A. Barker[1,5] and Haibo Lin[1,5,8*]

Abstract

Background This study reports the single-institution clinical experience of multifield pencil beam scanning (PBS) intensity-modulated proton therapy (IMPT) and dosimetric comparison to proton arc for uveal melanoma (UM) in a regular PBS gantry room.

Methods Eleven consecutive UM patients were treated with IMPT to 50 Gy in 5 fractions. A customized gaze-fixation device attached to the thermoplastic mask was used to reproduce the globe position for each patient. IMPT plans were robustly optimized with perturbations of 3 mm setup and 3.5% range uncertainties using 3–4 fields without apertures. Each plan was robustly reoptimized (using the same perturbation parameters) using two non-coplanar arc fields in the RayStation treatment planning system. Treatment quality for both plans was evaluated daily using CBCT-generated synthetic CT. Target coverage, conformity, and mean/maximum doses to adjacent organs were assessed.

Results Proton arc plans provided comparable plan quality compared to IMPT plans. Similar target coverage was achieved, with an average GTV D95% equal to 101.1% ± 1.0% and 101.4% ± 0.4% for IMPT and proton arc plans, respectively. Proton arc improves the conformity index (RTOG) compared to IMPT plans (average 0.96 ± 0.23 vs. 0.88 ± 0.18, $p = 0.11$). Both modalities met all the clinical goals for organs-at-risk (OARs), while proton arc significantly reduced the maximum dose for the retina from, on average, 54.5 ± 0.7 to 53.2 ± 0.3 Gy ($p < 0.01$). Treatment evaluation on synthetic CT showed that the doses received by patients were highly consistent with the planned doses, with a relative target coverage (D95%) difference within 3.5% for IMPT and 3.1% for proton arc, and the D95% of actual delivery exceeding 98.7% and 98.2%, respectively. The doses delivered to OARs did not exceed clinical constraints.

Conclusions This is a novel report on proton arc for ocular tumors and gantry-based multifield PBS proton treatment for these tumors. This study demonstrated that both modalities can meet the clinical goals. The IMPT is currently clinically implanted, and 2-field non-coplanar proton arc plans can achieve comparable dosimetric metrics to those of IMPT plans when the deliver technique is matured.

*Correspondence:
Haibo Lin
hlin@nyproton.com

Full list of author information is available at the end of the article

Keywords Uveal melanoma, Pencil beam scanning, Intensity modulated proton therapy, Proton arc therapy

Background

Uveal melanoma is the most common primary intraocular cancer in adults and is associated with significant morbidity and mortality [1, 2]. Earlier treatment methods relied on surgical removal of the eye (enucleation), accomplished at the cost of vision and quality of life. Other treatment modalities include eye-preserving therapies, such as radiotherapy. According to Collaborative Ocular Melanoma Studies (COMS), plaque brachytherapy can achieve excellent rates of preservation of vision without compromising survival rates [3, 4]. This advantage caused an increasing tendency for eye-preserving radiotherapy [5]. The limitations of plaque brachytherapy include a higher risk of recurrence, especially for larger tumors and those close to the optic disc [6, 7]. Proton beam therapy, however, is feasible for large tumors with challenging locations and/or shapes [8–12]. In practice, proton beam therapy can reduce the risks of retinopathy, local recurrence, and cataract formation [13].

The first application of proton beam therapy for uveal melanoma was in 1975 [14], and it is now used as a standard modality [11, 15, 16]. The vast majority of ocular proton therapy treatments to date have used passive scattering proton beams relying on a specific ocular treatment planning system, as well as a dedicated treatment room equipped with a fixed horizontal beamline and patient-specific aperture [17–19], thus contributing to the geospatial disparities in access to ocular proton therapy [20]. At the same time, the delivery technique of proton therapy has evolved significantly from passive scattering to pencil-beam scanning (PBS). PBS has demonstrated its universality and good performance in various disease sites with high precision and 3D dose conformity, which has led to an increasing number of proton centers worldwide equipped with PBS technology. Considering its potential improvements in plan quality and wider availability, it is promising to explore the feasibility of treating uveal melanoma using gantry-based PBS proton therapy.

In addition, with the development and increasing availability of proton PBS, proton arc therapy using the PBS technique is under investigation [21–25]. During proton arc therapy, the gantry rotates automatically around the patient within the start and stop angle. At the same time, an intensity-modulated proton beam is delivered to a series of optimized spot lists at different energy layers for each beam angle. With more degrees of freedom in this technique, proton arc therapy is expected to offer improved dose conformity. Previous studies have explored the clinical benefits of proton arc therapy for various disease sites [26–29]. Proton arc therapy can achieve comparable or better plan quality with respect to plan robustness, target conformity, organs-at-risk (OARs) sparing, and lower integral dose. It is highly desired to test PBS-based proton arc therapy for uveal melanoma, where the tumor is small and surrounded by various critical OARs such as the retina, optic nerve, cornea, lens, conjunctiva, eyebrow, and lacrimal gland.

This study demonstrates the treatment of uveal melanoma with proton PBS in a regular treatment room at our institute. The delivered doses to patients were evaluated by forwardly calculating each plan on synthetic CT of daily CBCT. We also explored the feasibility of proton arc therapy in the treatment of uveal melanoma.

Methods

Patient characteristics

With approval from the institutional review board, a cohort of 11 consecutive uveal melanoma patients treated with multiple-field PBS proton therapy using the ProBeam (Varian Medical Systems, Palo Alto, USA; arc delivery is currently not available) system in our institute was included in this study [30]. Table 1 shows the patients' characteristics, tumor dimensions, and the key planning parameters. All patients had a peripapillary/foveal tumor, adjacent to or overlapping with the optic nerve head/macula/fovea. The tumor size varied from 0.24 to 2.98 cc, with a median of 0.42 cc. Patients 2 and 3 received plaque brachytherapy (Pd-103) for the same disease site before the proton treatment. Radiation oncologists, ophthalmologists, medical dosimetrists, and physicists were involved in the institutional review of the treatment plan and included in the author list.

Intensity-modulated proton therapy

With diagnostic evaluation and confirmation from the ophthalmic oncology team and radiation oncology team, conventional intensity-modulated proton therapy (IMPT) prescribed to 50 Gy (relative biological effectiveness of 1.1) in 5 fractions was planned for each patient. Firstly, patients underwent surgical placement of tantalum fiducial markers on the sclera, and the marker positions were chosen to avoid potential proton trajectories and dose shadow effect [31]. The number of markers for each patient was 2–3. During CT simulation, a patient-specific thermoplastic head mask (Qfix, Avondale, PA, USA) attached with a customized gaze-fixation device was made to define the globe gazing position and reproduce the position for each treatment (Fig. 1 (A)). CT simulations (1.0 mm slice thickness was verified to achieve same dose calculation accuracy versus smaller thickness) were performed once the patients and ocular positions

Table 1 Characteristics of ocular patients and their treatment plans

Patient	Diseased eye /Prior RT	Tumor		Gantry angle-Couch angle-Range shifter (cm)	
		Volume [cc]	Diameter/Thickness [cm]	IMPT	Arc
1	Left/No	1.09	1.6/0.6	G325C0R0 G115C0R0 G135C0R0	Arc plan parameters are valid for all patients and only depend on the disease side (left/right). Left eye: G: 85–135 C: 30/330 R: 0 Right eye: G: 225–275 C: 30/330 R: 0
2	Right/Right	0.71	1.5/0.5	G30C0R0 G270C0R0 G270C90R0 G240C0R0	
3	Right/Right	0.77	1.5/0.2	G280C0R2 G270C30R2 G260C0R2 G240C0R2	
4	Left/No	0.30	1.0/0.3	G90C0R2 G125C0R2 G90C335R2	
5	Right/No	0.34	0.8/0.1	G300C0R3 G270C0R3 G240C0R3	
6	Right/No	2.98	2.5/0.4	G270C0R0 G250C0R0 G230C0R0 G230C40R0	
7	Left/No	0.30	0.8/0.5	G120C0R2 G90C330R2 G85C0R2	
8	Left/No	0.24	0.5/0.4	G120C0R2 G90C0R2 G90C330R2	
9	Right/No	0.42	1.0/0.6	G270C30R2 G265C0R2 G240C0R2	
10	Left/No	1.47	2.0/0.4	G125C0R2 G100C330R2 G250C90R0	
11	Right/No	0.38	1.0/0.4	G260C0R2 G250C0R2 G235C0R0	

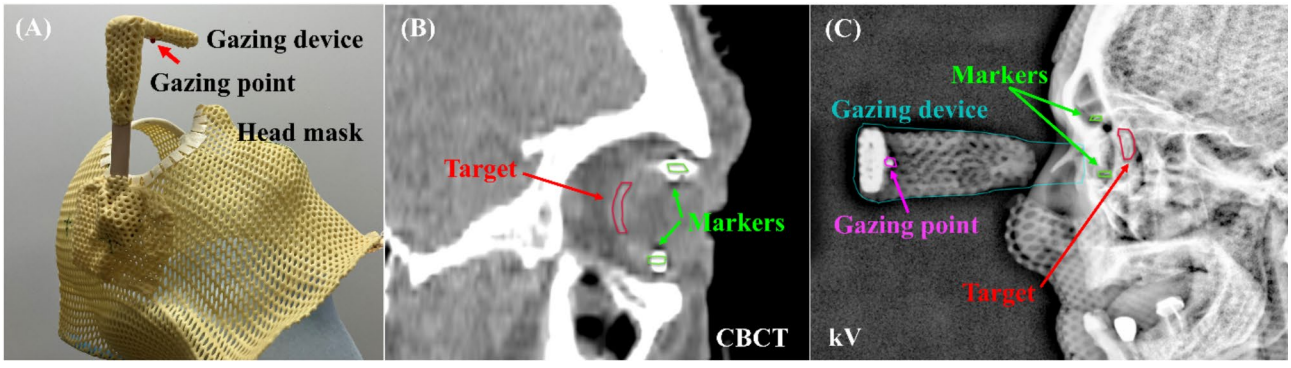

Fig. 1 (**A**) Patient-specific thermoplastic head mask attached with a customized gazing device. (**B**) CBCT and (**C**) kV images acquired for IGRT purpose, as well as the aligned contours of target, tantalum markers, gazing device and gazing point on them

were defined by the mentioned immobilization devices with eyes staring at the gaze point. Following CT simulation, and with the fundus mapping provided by ophthalmologist, the gross/clinical target volume (GTV/CTV) and OARs were contoured for plan optimization and evaluation. The tantalum markers and gazing device were also contoured, together with the 20% isodose volume, lens and optical nerves structures, as reference structures for image-guidance of daily treatment. Figure 1 shows the photos of the patient-specific head mask, the CBCT and kV images with aligned contours of target, tantalum markers, gazing device and gazing point on it.

The treatment plan was robustly optimized considering 3 mm setup and 3.5% range uncertainties [16] using the analytical algorithm in Eclipse V16.1 treatment planning system (TPS; Varian Medical Systems, Palo Alto, USA) to ensure that 95% of the GTV or CTV received at least 100% of the prescription dose and the maximum dose was within 110% of the prescription dose. Figure 2; Table 1 show the couch angle and gantry angle of the planned fields for each patient. Single-field optimization (each field provides uniform target coverage) with 3 fields was applied for most cases. Multifield optimization (flexible field dose, but the sum dose provides uniform target coverage) and/or 4 fields were used for patients 1 and 6, whose tumors had a relatively large size or concave shape, and patients 2 and 3 due to their cases being reirradiation and a need to achieve higher conformity and OAR sparing [32]. A gantry-mounted range shifter with 2–3 cm water-equivalent-thickness was used for fields with a shallow tumor depth in the plan optimization [33] (no range shifter was used for patients 1, 2, and 6). The dose calculation was independently verified using AcurosPT V16.1, which is a Monte Carlo algorithm in Eclipse TPS [34], with a dose grid of 1 mm.

Proton arc therapy

As Eclipse TPS doesn't provide a proton arc planning function, treatment plans were reoptimized on the planning CT using two non-coplanar arc fields in the research version of the RayStation 2023B TPS (RaySearch Laboratories AB, Stockholm, Sweden), which has been validated against measurements and Eclipse TPS during commissioning. Since the dose calculation and treatment does not involve an aperture or low-density tissue such as lung, deviations between calculation algorithms should not impact the results. The ELSA (Early Layer and Spot Assignment) algorithm was used in arc plan optimization [21]. The algorithm assigns spots to a single energy layer per discretized direction before spot weight optimization and reduces the number of initial spots considerably compared to conventional methods. The clinical goals, prescribed target dose, dose grid, and robust optimization parameters were the same as the IMPT plan. In addition, anterior beams were avoided to minimize the dose to the anterior segment of the eye, eliminate the use of an eye retractor, and reduce potential range uncertainty induced by the eyelid. Posterior and vertex

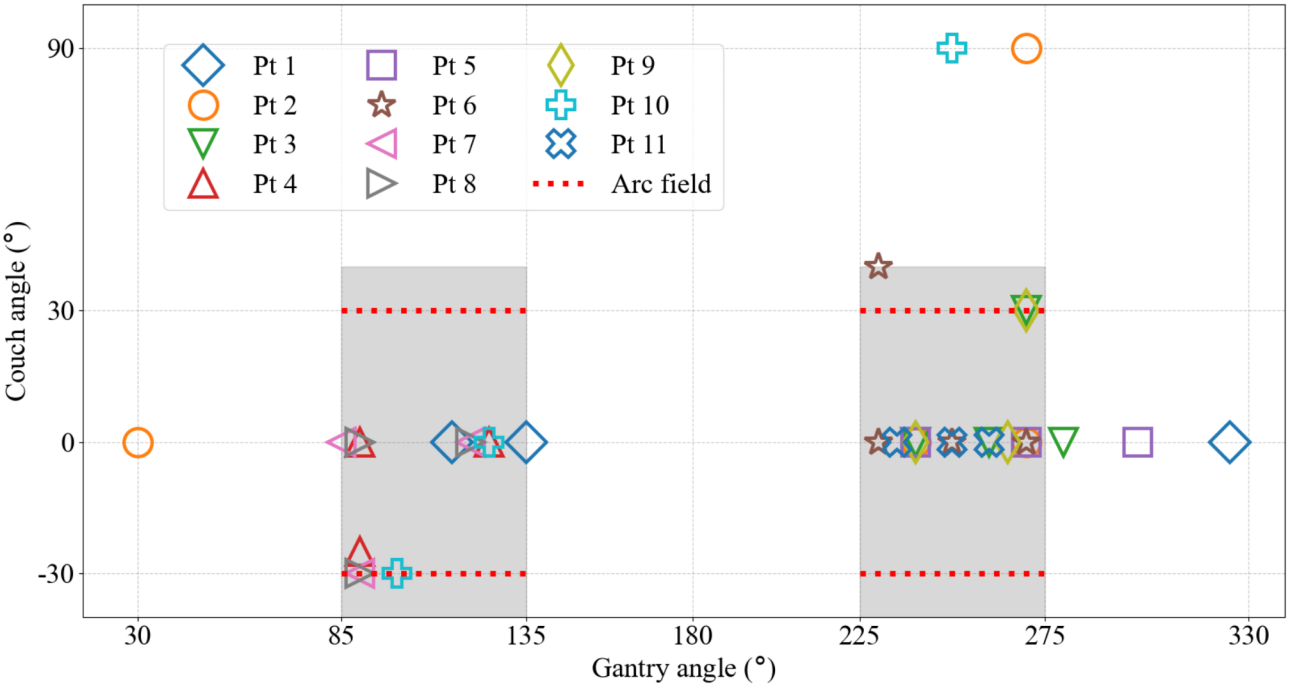

Fig. 2 Couch angle and gantry angle of the planned fields for each patient. Dotted lines represent the arc fields in the proton arc plan. Gray shadows represent the favorable zone of field angles, i.e. lateral and lateral posterior oblique on the target side

beams, which may raise the radiation risk for the brain due to the entrance dose, were also avoided. The use of a range shifter was avoided to maintain the spot size and reduce the penumbra. The gantry rotation starts from 85° to 135° (225° to 275°) for the left (right) diseased eye, and the number of directions for each beam was 30. For each plan, the couch angle was 30° (330°) for the first (second) arc field. The arc fields avoided tantalum markers. The plans were optimized and calculated using RayStation's Monte Carlo algorithm, which uses 30,000 particles and has a statistical uncertainty of 1.0%.

Plan evaluation

Plan evaluation was performed with the following dosimetric metrics: the dose that covers 95% of the target volume (D95%), the conformity index as proposed by the Radiation Therapy Oncology Group (RTOG) i.e. CI_{RTOG} = V95%/TV, where V95% represents 95% of the prescribed isodose volume, TV represents the volume of the target with 3 mm isometric expansion [35], R50% = V50%/TV and R10% = V10%/TV, mean/maximum doses to critical OARs (D_{mean}/D_{max}), including the retina, optic nerve, cornea, lens, conjunctiva, eyebrow, and lacrimal gland. Considering these are all peripapillary/foveal tumors, other organs are not involved due to their overlapping with the tumor or OARs. The proton arc plan was normalized to match the target coverage with IMPT plan based on metrics of D95%. The numbers of spots and energy layers were also compared. To evaluate the plan's robustness against the uncertainties in daily treatment, synthetic CTs generated with daily CBCTs as well as the corresponding image registrations between planning CT during treatment were used for plan forward calculation to estimate the dose delivered to the patient [36]. Dosimetric comparison was performed in two aspects: inter-plan comparison between proton arc and IMPT plans, and intra-plan comparison between planned dose and dose delivered to patient. A paired 2-tailed t-test using the SciPy package in Python was performed [37]. A p-value less than 0.05 was considered statistically significant.

Results

Inter-plan comparison

The total number of energy layers for all fields for proton arc plan was significantly higher than for IMPT plan (average 470 ± 120 vs. 51 ± 20, $p < 0.01$), and the total number of spots was comparable (average 1822 ± 1928 vs. 2258 ± 1302, $p = 0.51$). Figure 3 shows the comparison of dose distributions and dose-volume histograms (DVHs) for a representative patient (patient 5). For this patient, the gantry angles of 300°, 270° and 240° were used for the IMPT plan with a couch angle of 0°, and gantry angles from 225° to 275° were used for the arc plan with couch angles of $\pm 30^\circ$. Across the cohort, based on DVHs comparison, the target coverage was comparable between two modalities, and the proton arc plan trended toward a better conformity to the GTV. Proton arc plans maintained the dose constraints to OARs.

Figure 4 shows a box plot of maximum (A) and mean (B) doses to OARs for the IMPT and proton arc plans of all patients in this study. As shown in Fig. 4 (A), the upper limits of the maximum dose from proton arc plans were lower than IMPT plans for most of the OARs. This was particularly notable for the maximum dose to the retina for patient 1, which was 56.0 Gy, exceeding the clinical constraint of 55 Gy, whereas the goal was achieved by the proton arc plan (53.3 Gy).

Table 2 summarizes the averaged numerical result of dosimetric metrics from all patients for the two modalities. The plan quality of proton arc plans was consistent with IMPT plans. Similar target coverage was achieved by proton arc and IMPT plans with D95% equal to 101.4% ± 0.4% and 101.1% ± 1.0%, respectively. Proton arc plans trended toward better conformity index compared to IMPT plans, with CI_{RTOG} equals to 0.96 ± 0.23 and 0.88 ± 0.18 ($p = 0.11$), respectively, with comparable R50% (7.25 ± 1.98 vs. 7.24 ± 2.12, $p = 0.97$) and significantly higher R10% (50.71 ± 16.89 vs. 41.83 ± 13.80, $p = 0.01$). Proton arc and IMPT plans showed comparable performance on OAR sparing with respect to the dosimetric metrics of maximum/mean doses to most OARs (Table 2). Proton arc plans, however, significantly reduced the maximum dose for the retina, with the average value decreased from 54.5 ± 0.7 to 53.2 ± 0.3 Gy ($p < 0.01$). No significant differences were found for other metrics and OARs.

Intra-plan comparison

The dosimetric difference between the planned dose and the dose delivered to the patient was compared for both modalities. Figure 4 shows the box plot of maximum (A) and mean (B) doses to OARs from plan and delivery. In general, the treatment delivery maintained the dosimetric quality for both plans with respect to the clinical goals for target coverage and OAR constraints. Both planning and treatment evaluations resulted in GTV D95% higher than 98.7% and 98.2% for IMPT and proton arc, respectively. Figure 5 shows the box plot of the relative differences between dose metrics from delivery (D_{Eval}) and plan (D_{Plan}) for these two modalities. For IMPT plans, the relative differences on GTV D95% were within 3.5%, and the worst case was patient 4 with GTV D95% decreasing from 102.3% (plan) to 98.7% (delivery). For proton arc plans, the relative differences were within 3.1%, and the worst case was patient 7 with GTV D95% decreased from 101.3% (plan) to 98.2% (delivery). The relative differences in the maximum dose of the retina were significantly

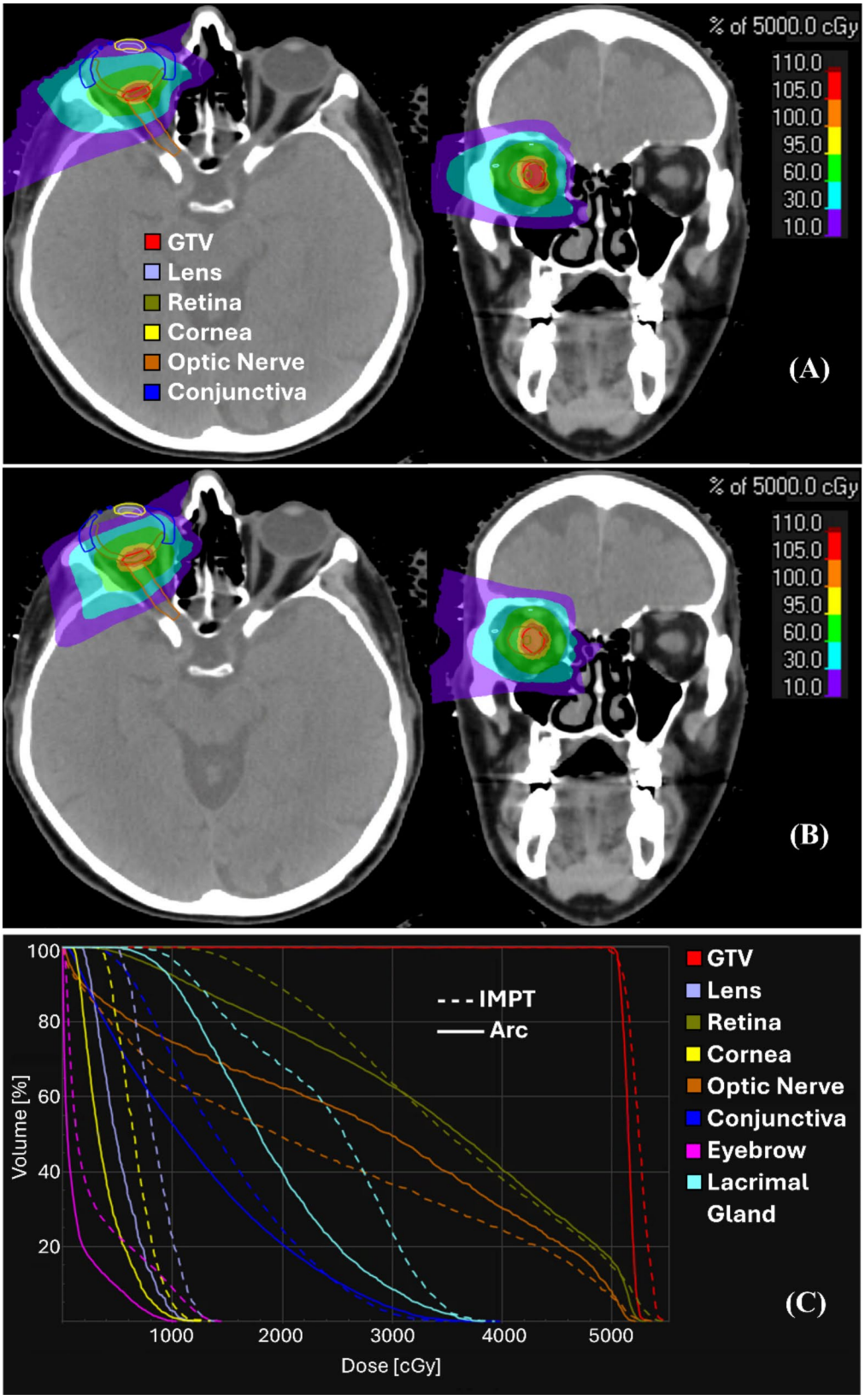

Fig. 3 Comparison of dose distributions of the IMPT plan (**A**) and proton arc plan (**B**) for a representative patient (patient 5), as well as the corresponding DVHs (**C**), in which solid lines represent proton arc plan and dashed lines represent IMPT plan. The red contour in CT (**A**, **B**) represents GTV

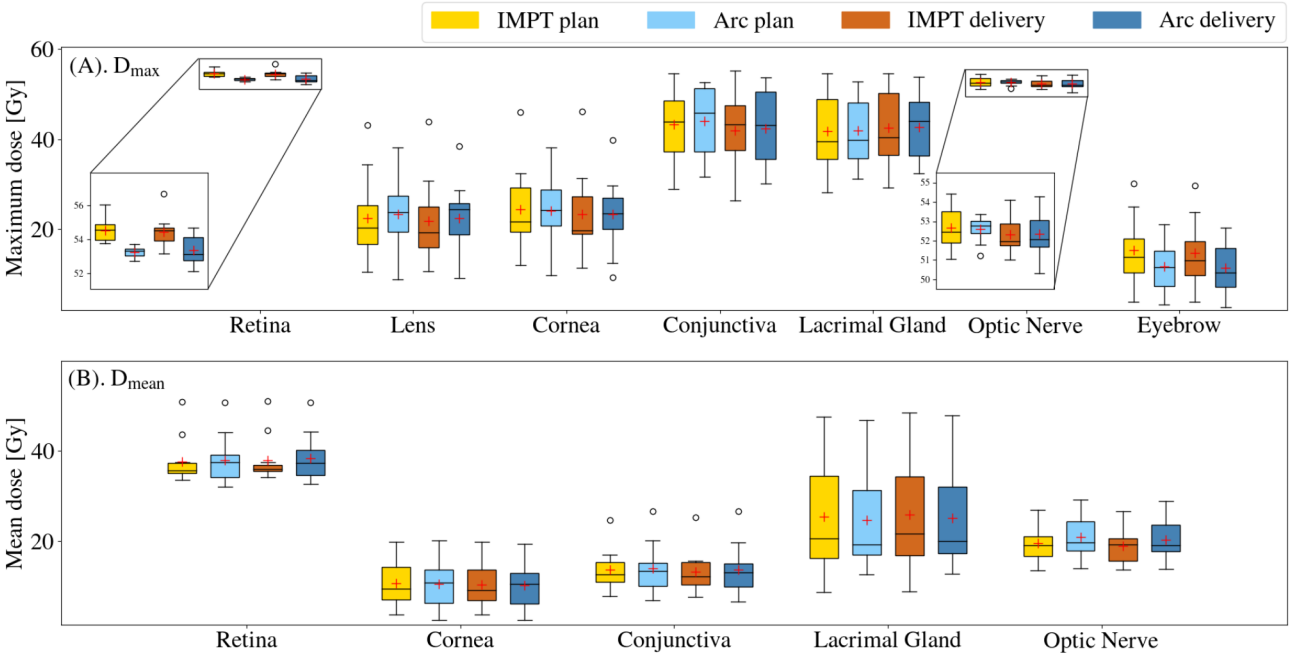

Fig. 4 Box plot of the maximum (**A**) and mean (**B**) doses to OARs from the IMPT plans and proton arc plans, as well as the corresponding delivery results. The red cross represents the mean value. The circles outside of the box are outliers

Table 2 Comparison of the averaged numerical result of dosimetric metrics from all patients for target coverage and dose to oars between IMPT and proton Arc plans

		Clinical goal	IMPT plan	Arc plan	*p*-value
GTV	D95% [%]	> 100	101.1 ± 1.0	101.4 ± 0.4	0.29
	CI_{RTOG}	1	0.88 ± 0.18	0.96 ± 0.23	0.11
	R50% [%]		7.24 ± 2.12	7.25 ± 1.98	0.97
	R10% [%]		41.83 ± 13.80	50.71 ± 16.89	0.01
Retina	D_{max} [Gy]	< 55	54.5 ± 0.7	53.2 ± 0.3	< 0.01
	D_{mean} [Gy]		37.7 ± 4.9	38.0 ± 5.2	0.66
Lens	D_{max} [Gy]	< 30	22.4 ± 9.2	23.4 ± 8.0	0.42
Cornea	D_{max} [Gy]	< 30	24.4 ± 9.1	24.0 ± 7.7	0.82
	D_{mean} [Gy]		10.7 ± 5.5	10.5 ± 5.4	0.81
Conjunctiva	D_{max} [Gy]	< 55	43.2 ± 7.9	44.0 ± 7.5	0.30
	D_{mean} [Gy]		13.6 ± 4.6	14.0 ± 5.7	0.77
Lacrimal Gland	D_{max} [Gy]	< 55	41.8 ± 8.6	41.9 ± 7.3	0.92
	D_{mean} [Gy]		25.5 ± 12.5	24.6 ± 12.2	0.61
Optic Nerve	D_{max} [Gy]	< 55	52.7 ± 1.1	52.6 ± 0.6	0.86
	D_{mean} [Gy]		19.6 ± 4.0	21.0 ± 4.6	0.10
Eyebrow	D_{max} [Gy]	< 20	15.3 ± 7.9	11.7 ± 5.8	0.13

larger for proton arc plans (0.7% ± 0.6%) compared to IMPT plans (-0.2% ± 0.6%). The doses received by OARs from delivery met the requirements of the dose constraints. The evaluation results confirmed the robustness of the IMPT and proton arc plans against the uncertainties in daily treatment, as well as the reproducibility of daily treatments with the presented treatment modality.

Discussion

Ocular tumors are mostly treated with eye-preserving radiotherapy, such as plaque brachytherapy, which is mostly used for tumors in the iris/ciliary body [8]. Previous studies show that, with a combination of dynamic conformal arcs and intensity-modulated static fields, stereotactic photon radiotherapy can achieve highly conformal dose distribution and good OAR-sparing for ocular patients [38]. For larger peripapillary/foveal tumors, proton beam therapy is preferred. Although proton therapy has shown good outcomes in treating ocular cancers, the

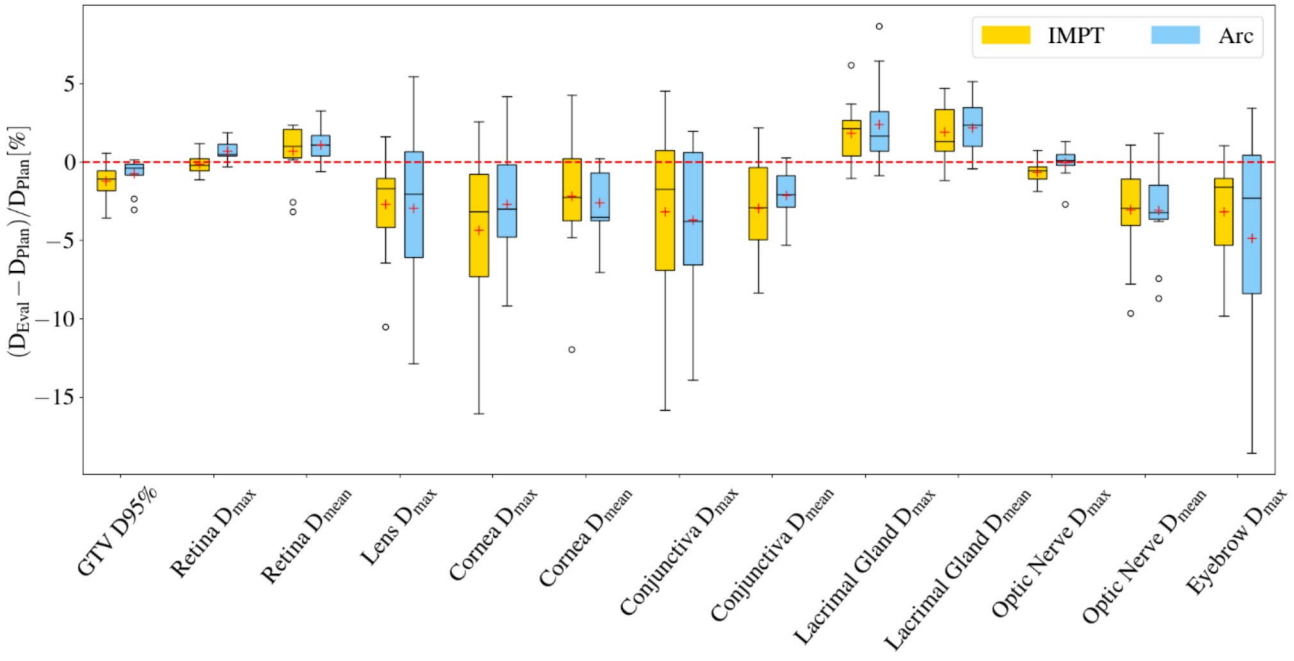

Fig. 5 Box plot of relative differences between dose metrics from delivery (D_{Eval}) and plan (D_{Plan}) for proton arc (blue) and IMPT (yellow)

availability of dedicated eye beamlines is limited due to the relatively low disease population [16]. In this case, a regular proton PBS-gantry system could be an alternative treatment option for ocular patients.

The PBS technique has developed rapidly in recent years. It is an intricate, personalized proton beam delivery technology that can customize the dose distribution to precisely conform to the target without the need for a patient-specific aperture. Combining the IMPT plans generated with 3D CT images and an advanced treatment planning system with image-guided alignment, PBS proton therapy has shown good performance and universality in the treatment of various disease sites [38].

Proton arc therapy is an advanced treatment technology. Compared with conventional IMPT, which uses multiple static fields, proton arc therapy is operated by rotating the gantry continuously and delivering the proton beams to the tumor simultaneously. With more degrees of freedom, proton arc therapy has the potential to compete with IMPT. Previous studies showed comparable or better plan quality can be achieved with proton arc, and dosimetric improvements include target coverage, plan robustness, lower integral dose and lower skin or entrance dose. In addition, with the development of a proton machine on the energy layer switch time and gantry rotation time, less delivery time can potentially be achieved with a proton arc compared to IMPT, especially for an IMPT plan with more than two fields [39], addition time is needed between field to adjust gantry angle and request beam. Proton arc therapy can reduce pause time during delivery and could take advantage of the gantry rotation time to switch energy, which may significantly reduce the treatment time.

In this study, we demonstrated that IMPT operated in a regular gantry room for the treatment of uveal melanoma is feasible. We also demonstrated that proton arc therapy based on the PBS technique can achieve a plan quality that is comparable with or even improved relative to IMPT. According to previous experiences [17, 40, 41], hypo-fractionated proton therapy is preferred for uveal melanoma but requires a high degree of setup accuracy. All patients in this study completed their treatment in five separate days. Daily kV and CBCT images were acquired for patient alignment, especially on the position of the gaze point, bone anatomy, and tantalum marker of the eye. Plan evaluation results showed that, with the usage of immobilization devices and image-guided alignment, daily delivery quality and reproducibility can be ensured.

The ocular region is a challenging disease site, with many critical OARs and limited space between OARs and tumor. OAR sparing with proton therapy can be optimized in two ways: minimizing the proximal dose and the lateral dose to OARs. In this study, the patients are all with peripapillary/foveal tumors. The optic disc and fovea/macula typically receive the full prescription dose, therefore, the radiation oncologist didn't draw those structures or add dose constraints. The ciliary body is a small structure and closely approximated lens. In CT, accurately delineating the ciliary body is a challenge. To limit secondary glaucoma toxicities, dose constraints to the lens are a good alternative way [42]. To minimize

the proximal dose to OARs, favorable beam directions are the lateral and lateral posterior oblique region of the ipsilateral side. As shown in Fig. 2, to achieve the clinical goals, this requirement was not successfully addressed by several fields of IMPT plans for the following patients (gantry angle, couch angle): patient 1 (325, 0), patient 2 (30, 0; 270, 90), and patient 10 (250, 90). They received anterior or vertex fields, which raises the radiation risk for the lens, cornea, conjunctiva, and brain, as well as the uncertainty from the eyelid. On the other hand, all proton arc plans had a universal field arrangement with beam directions within the favorable regions. For the IMPT plan, to reach the superficial region of the tumor, a range shifter was needed for a portion of the fields, which will widen the beam penumbra, thus increasing the lateral dose of OARs. In proton arc plans, the range shifter can be avoided, and the superficial spots can be reached from other beam directions [26].

In the treatment of small tumors with a high dose in a few fractions, special attention should be paid to dosimetric accuracy and reproducibility. In this study, the median tumor size was 0.42 cc. Small errors in dose distribution or patient alignment can induce a relatively large influence on plan quality. To ensure dosimetric accuracy, the treatment machine and dose delivery accuracy were validated for small field (D50% $\leq$ 2.5 cm) irradiation. The spot size was measured at every 5-degree gantry angle. The spot size variations were within 10% for each energy at different gantry angles. Monte Carlo-based treatment planning, as well as robust optimization, is recommended to achieve a better estimation of the dose delivery [43]. Quality assurance should consider the relatively shallow tumor depth and the necessity of a high spatial resolution detector [44]. During daily treatment, customized immobilization devices and advanced image-guidance techniques should be used for reproducibility. CBCT devices mounted on the gantry can provide 3D anatomic information for a patient in the treatment position [45]. It can efficiently reconstruct the contours of soft tissue, bone, and artificial marker with high resolution and is widely used in image-guided radiotherapy [46]. In addition, to further improve the dosimetric accuracy and reproducibility, potential solutions are the application of a beam-specific aperture that can increase the beam gradient [47], and an eye-tracking device that can ensure the alignment during beam delivery (24 $\pm$ 10 second duration) [48].

This study has limitations on field arrangement to fully explore the potential of arc delivery. Previous studies have shown that superior dosimetric quality can be achieved with more arc fields, and for the disease sites that can be treated with a full arc field, dosimetric quality can be improved significantly compared to IMPT [21, 26, 29, 39, 49, 50, 51]. In addition, with more arc fields, proton arc therapy has the potential to optimize the distribution of dose-averaged linear energy transfer, resulting in higher radiobiological effectiveness inside of the target and lower normal tissue toxicity [52, 53]. It should be noted that, for the treatment of uveal melanoma, due to the aforementioned requirements on field angle selection, it is hard to further explore the potential of proton arc therapy with more arc fields based on the current machine design. A potential solution would be to include more couch angles or dynamic couch rotation during the treatment delivery [54]. Currently, arc delivery is not available for most proton machines. To establish proton arc treatment as a clinically viable option, further advancements are required to improve the efficiency of robust plan optimization. Additionally, developing a reliable delivery system capable of delivering precise beam and highly reproducible dosimetry, combined with rapid energy modulation and seamless dynamic gantry rotation, is essential for successfully implementing proton arc delivery. Nevertheless, proton arc therapy can simplify manual intervention and advance radiotherapy further in the direction of automation.

Conclusions

This study investigated the potential of using proton arc treatment for ocular disease and compared it to the multiple-field IMPT treatment. An efficient worldwide available solution based on a regular proton PBS-gantry room for the treatment of uveal melanoma was presented. With the assistance of an immobilization device and precise image-guided patient alignment, IMPT delivered with PBS for the treatment of uveal melanoma is feasible with high reproducibility. This study also demonstrated, for the first time, that two-field non-coplanar proton arc therapy can achieve comparable dosimetric metrics to those of IMPT plans for ocular tumors, reducing the retina's maximum dose.

Abbreviations

CI	Conformity index
COMS	Collaborative ocular melanoma studies
D95%/D50%	Dose that covers 95%/50% of the target volume
D_{Eval}/D_{Plan}	Dose metrics from evaluation/plan
D_{mean}/D_{max}	Mean/maximum dose to OARs
DVHs	Dose-volume histograms
GTV/CTV	Gross/clinical target volume
IMPT	Intensity-modulated proton therapy
OARs	Organs-at-risk
PBS	Pencil beam scanning
R50%/R10%	V50%/V10% divided by TV
RTOG	Radiation therapy oncology group
TPS	Treatment planning system
TV	Volume of the target with 3 mm isometric expansion
UM	Uveal melanoma
V95%/V50%/V10%	The 95%/50%/10% prescribed isodose volume

Acknowledgements

Research funding support, in part, by Varian Medical System (Palo Alto, USA) and NIH/NCI Cancer Center Support Grant P30 CA008748.

Author contributions
H.Q. and H.L. are responsible for the study concept, plan optimization and wrote the main manuscript. H.Q. acquired and analyzed the data. L.H., S.H., Y.P.L, D.H.A, J.H.F and C.A.B reviewed and selected the patients. F.Y, Q.C., Y.Y., M.K., H.Z., A.S., P.P., X.D., J.Z, D.H.A, J.H.F, C.B.S, C.A.B and H.L. reviewed the plan. M.V., L.H., X.D., J.Z., C.B.S, D.H.A, J.H.F, C.A.B and H.L. edited the manuscript. All authors reviewed the manuscript.

Funding
Varian Medical System (Palo Alto, USA) Research Grant.
NIH/NCI Cancer Center Support Grant P30 CA008748.

Data availability
No datasets were generated or analysed during the current study.

Declarations

Ethics approval and consent to participate
Not applicable.

Consent for publication
Not applicable.

Competing interests
The authors declare no competing interests.

Author details
[1]New York Proton Center, New York, NY, USA
[2]Inova Schar Cancer Institute, Fairfax, VA, USA
[3]Tianjin Medical University Cancer Institute and Hospital, Tianjin, China
[4]University of Iowa Health Care, Iowa City, IA, USA
[5]Memorial Sloan Kettering Cancer Center, New York, NY, USA
[6]William Beaumont University Hospital, Corewell Health, Royal Oak, MI, USA
[7]Emory University, Atlanta, GA, USA
[8]Department of Radiation Oncology, Albert Einstein College of Medicine and Montefiore Medical Center, Bronx, NY, USA

Received: 17 November 2024 / Accepted: 10 March 2025
Published online: 02 April 2025

References

1. Kaliki S, Shields CL. Uveal melanoma: relatively rare but deadly cancer. Eye. 2017;31:241–57.
2. Rantala ES, Hernberg M, Kivelä TT. Overall survival after treatment for metastatic uveal melanoma: a systematic review and meta-analysis. Melanoma Res. 2019;29:561.
3. Collaborative Ocular Melanoma Study Group. The COMS randomized trial of iodine 125 brachytherapy for choroidal melanoma: V. Twelve-year mortality rates and prognostic factors: COMS report No. 28. Archives of ophthalmology (Chicago, Ill.: 1960), 2006;124(12):1684–1693.
4. Wisely CE, Hadziahmetovic M, Reem RE, Hade EM, Nag S, Davidorf FH, et al. Long-term visual acuity outcomes in patients with uveal melanoma treated with 125I episcleral OSU-Nag plaque brachytherapy. Brachytherapy. 2016;15:12–22.
5. Tarlan B, Kıratlı H. Uveal melanoma: current trends in diagnosis and management. Turkish J Ophthalmol. 2016;46:123.
6. Zemba M, Dumitrescu O-M, Gheorghe AG, Radu M, Ionescu MA, Vatafu A, Dinu V. Ocular complications of radiotherapy in uveal melanoma. Cancers. 2023;15:333.
7. Karimi S, Arabi A, Siavashpour Z, Shahraki T, Ansari I. Efficacy and complications of ruthenium-106 brachytherapy for uveal melanoma: a systematic review and meta-analysis. J Contemp Brachytherapy. 2021;13:358–64.
8. Damato BE. Treatment selection for uveal melanoma. Curr Concepts Uveal Melanoma. 2012;49:16–26.
9. Marucci L, Ancukiewicz M, Lane AM, Collier JM, Gragoudas ES, Munzenrider JE. Uveal melanoma recurrence after fractionated proton beam therapy: comparison of survival in patients treated with reirradiation or with enucleation. Int J Radiation Oncology* Biology* Phys. 2011;79:842–6.
10. Weber B, Paton K, Ma R, Pickles T. Outcomes of proton beam radiotherapy for large non-peripapillary choroidal and ciliary body melanoma at TRIUMF and the BC cancer agency. Ocular Oncol Pathol. 2015;2:29–35.
11. Foti PV, Travali M, Farina R, Palmucci S, Spatola C, Liardo RLE, et al. Diagnostic methods and therapeutic options of uveal melanoma with emphasis on MR imaging—part II: treatment indications and complications. Insights into Imaging. 2021;12:1–24.
12. Grech Fonk L, Ferreira TA, Webb AG, Luyten GPM, Beenakker JM. The economic value of MR-imaging for uveal melanoma. Clinical ophthalmology (Auckland, N.Z.), 2020;14:1135–1143.
13. Wang Z, Nabhan M, Schild SE, Stafford SL, Petersen IA, Foote RL, Murad MH. Charged particle radiation therapy for uveal melanoma: a systematic review and meta-analysis. Int J Radiation Oncology* Biology* Phys. 2013;86:18–26.
14. Gragoudas ES, Goitein M, Koehler AM, Verhey L, Tepper J, Suit HD, et al. Proton irradiation of small choroidal malignant melanomas. Am J Ophthalmol. 1977;83:665–73.
15. Aziz S, Taylor A, McConnachie A, Kacperek A, Kemp E. Proton beam radiotherapy in the management of uveal melanoma: Clinical experience in Scotland. Clin Ophthalmol. 2009;3:49–55.
16. Hrbacek J, Kacperek A, Beenakker JM, Mortimer L, Denker A, Mazal A, Shih HA, Dendale R, Slopsema R, Heufelder J, Mishra KK, Hrbacek J, Kacperek A, Beenakker JM, Mortimer L, Denker A, Mazal A, Shih HA, Dendale R, Slopsema R, Heufelder J, Mishra KK. PTCOG ocular statement: Expert summary of current practices and future developments in ocular proton therapy. Int J Radiation Oncol Biol Phys. 2024;120(5):1307–1325.
17. Hrbacek J, Mishra KK, Kacperek A, Dendale R, Nauraye C, Auger M, et al. Practice patterns analysis of ocular proton therapy centers: the international OPTIC survey. Int J Radiation Oncology* Biology* Phys. 2016;95:336–43.
18. Slopsema R, Mamalui M, Zhao T, Yeung D, Malyapa R, Li Z. Dosimetric properties of a proton beamline dedicated to the treatment of ocular disease. Med Phys. 2014;41:011707.
19. Tran E, Ma R, Paton K, Blackmore E, Pickles T. Outcomes of proton radiation therapy for peripapillary choroidal melanoma at the BC cancer agency. Int J Radiation Oncology* Biology* Phys. 2012;83:1425–31.
20. Maillie L, Lazarev S, Simone CB, Sisk M. Geospatial disparities in access to proton therapy in the continental United States. Cancer Invest. 2021;39:582–8.
21. Engwall E, Battinelli C, Wase V, Marthin O, Glimelius L, Bokrantz R, et al. Fast robust optimization of proton PBS arc therapy plans using early energy layer selection and spot assignment. Phys Med Biol. 2022;67:065010.
22. Ding X, Li X, Zhang JM, Kabolizadeh P, Stevens C, Yan D. Spot-scanning proton arc (SPArc) therapy: the first robust and delivery-efficient spot-scanning proton arc therapy. Int J Radiation Oncology* Biology* Phys. 2016;96:1107–16.
23. Seco J, Gu G, Marcelos T, Kooy H, Willers H. Proton arc reduces range uncertainty effects and improves conformality compared with photon volumetric modulated arc therapy in stereotactic body radiation therapy for non-small cell lung cancer. Int J Radiation Oncology* Biology* Phys. 2013;87:188–94.
24. Sanchez-Parcerisa D, Kirk M, Fager M, Burgdorf B, Stowe M, Solberg T, Carabe A. Range optimization for mono-and bi-energetic proton modulated arc therapy with pencil beam scanning. Phys Med Biol. 2016;61:N565.
25. Liu G, Li X, Zhao L, Zheng W, Qin A, Zhang S, et al. A novel energy sequence optimization algorithm for efficient spot-scanning proton arc (SPArc) treatment delivery. Acta Oncol. 2020;59:1178–85.
26. Li X, Kabolizadeh P, Yan D, Qin A, Zhou J, Hong Y, et al. Improve dosimetric outcome in stage III non-small-cell lung cancer treatment using spot-scanning proton arc (SPArc) therapy. Radiat Oncol. 2018;13:1–9.
27. Chang S, Liu G, Zhao L, Dilworth JT, Zheng W, Jawad S, et al. Feasibility study: spot-scanning proton arc therapy (SPArc) for left-sided whole breast radiotherapy. Radiat Oncol. 2020;15:1–11.
28. Tattenberg S, Liu P, Mulhem A, Cong X, Thome C, Ding X. Impact of and interplay between proton arc therapy and range uncertainties in proton therapy for head-and-neck cancer. Phys Med Biol. 2024;69(5). https://doi.org/10.1088/1361-6560/ad2718.
29. de Jong BA, Korevaar EW, Maring A, Werkman CI, Scandurra D, Janssens G, et al. Proton arc therapy increases the benefit of proton therapy for oropharyngeal cancer patients in the model based clinic. Radiother Oncol. 2023;184:109670.
30. Langner UW, Eley JG, Dong L, Langen K. Comparison of multi-institutional varian probeam pencil beam scanning proton beam commissioning data. J Appl Clin Med Phys. 2017;18:96–107.

31. Newhauser WD, Koch NC, Fontenot JD, Rosenthal SJ, Gombos DS, Fitzek MM, Mohan R. Dosimetric impact of tantalum markers used in the treatment of uveal melanoma with proton beam therapy. Phys Med Biol. 2007;52:3979.
32. Yeung D, McKenzie C, Indelicato DJ. A dosimetric comparison of intensity-modulated proton therapy optimization techniques for pediatric craniopharyngiomas: a clinical case study. Pediatr Blood Cancer. 2014;61:89–94.
33. Shirey RJ, Wu HT. Quantifying the effect of air gap, depth, and range shifter thickness on TPS dosimetric accuracy in superficial PBS proton therapy. J Appl Clin Med Phys. 2018;19:164–73.
34. Lin L, Huang S, Kang M, Hiltunen P, Vanderstraeten R, Lindberg J, et al. A benchmarking method to evaluate the accuracy of a commercial proton Monte Carlo pencil beam scanning treatment planning system. J Appl Clin Med Phys. 2017;18:44–9.
35. Feuvret L, Noël G, Mazeron J-J, Bey P. Conformity index: a review. Int J Radiation Oncology* Biology* Phys. 2006;64:333–42.
36. Tsai P, Tseng Y-L, Shen B, Ackerman C, Zhai HA, Yu F, et al. The applications and pitfalls of cone-beam computed tomography-based synthetic computed tomography for adaptive evaluation in pencil-beam scanning proton therapy. Cancers. 2023;15:5101.
37. Virtanen P, Gommers R, Oliphant TE, Haberland M, Reddy T, Cournapeau D, et al. SciPy 1.0: fundamental algorithms for scientific computing in python. Nat Methods. 2020;17:261–72.
38. Kaiser A, Eley JG, Onyeuku NE, Rice SR, Wright CC, McGovern NE, Sank M, Zhu M, Vujaskovic Z, Simone CB 2nd, Hussain A. Proton therapy delivery and its clinical application in select solid tumor malignancies. J Visual Experiment. 2019;JoVE(144). https://doi.org/10.3791/58372.
39. Ding X, Li X, Qin A, Zhou J, Yan D, Stevens C, et al. Have we reached proton beam therapy dosimetric limitations?–a novel robust, delivery-efficient and continuous spot-scanning proton arc (SPArc) therapy is to improve the dosimetric outcome in treating prostate cancer. Acta Oncol. 2018;57:435–7.
40. Dendale R, Lumbroso-Le Rouic L, Noel G, Feuvret L, Levy C, Delacroix S, et al. Proton beam radiotherapy for uveal melanoma: results of curie Institut–Orsay proton therapy center (ICPO). Int J Radiation Oncology* Biology* Phys. 2006;65:780–7.
41. Caujolle J-P, Mammar H, Chamorey E, Pinon F, Herault J, Gastaud P. Proton beam radiotherapy for uveal melanomas at nice teaching hospital: 16 years' experience. Int J Radiation Oncology* Biology* Phys. 2010;78:98–103.
42. Mishra KK, Daftari IK, Weinberg V, Cole T, Quivey JM, Castro JR, et al. Risk factors for neovascular glaucoma after proton beam therapy of uveal melanoma: a detailed analysis of tumor and dose–volume parameters. Int J Radiation Oncology* Biology* Phys. 2013;87:330–6.
43. Bednarz B, Daartz J, Paganetti H. Dosimetric accuracy of planning and delivering small proton therapy fields. Phys Med Biol. 2010;55:7425.
44. McAuley GA, Teran AV, Slater JD, Slater JM, Wroe AJ. Evaluation of the dosimetric properties of a diode detector for small field proton radiosurgery. J Appl Clin Med Phys. 2015;16:51–64.
45. Jaffray DA, Siewerdsen JH, Wong JW, Martinez AA. Flat-panel cone-beam computed tomography for image-guided radiation therapy. Int J Radiation Oncology* Biology* Phys. 2002;53:1337–49.
46. Oldham M, Létourneau D, Watt L, Hugo G, Yan D, Lockman D, et al. Cone-beam-CT guided radiation therapy: a model for on-line application. Radiother Oncol. 2005;75:271. E1-. E8.
47. Regmi R, Maes D, Nevitt A, Toltz A, Leuro E, Chen J, et al. Treatment of ocular tumors through a novel applicator on a conventional proton pencil beam scanning beamline. Sci Rep. 2022;12:4648.
48. Dieckmann K, Bogner J, Georg D, Zehetmayer M, Kren G, Pötter R. A linac-based stereotactic irradiation technique of uveal melanoma. Radiother Oncol. 2001;61:49–56.
49. Lee T-F, Ting H-M, Chao P-J, Fang F-M. Dual arc volumetric-modulated arc radiotherapy (VMAT) of nasopharyngeal carcinomas: a simultaneous integrated boost treatment plan comparison with intensity-modulated radiotherapies and single arc VMAT. Clin Oncol. 2012;24:196–207.
50. Zhao LR, Zhou YB, Sun JG. Comparison of plan optimization for single and dual volumetric-modulated arc therapy versus intensity-modulated radiation therapy during post-mastectomy regional irradiation. Oncol Lett. 2016;11:3389–94.
51. Ding X, Zhou J, Li X, Blas K, Liu G, Wang Y, et al. Improving dosimetric outcome for hippocampus and cochlea sparing whole brain radiotherapy using spot-scanning proton arc therapy. Acta Oncol. 2019;58:483–90.
52. Bertolet A, Carabe A. Proton monoenergetic arc therapy (PMAT) to enhance LETd within the target. Phys Med Biol. 2020;65:165006.
53. Li X, Ding X, Zheng W, Liu G, Janssens G, Souris K, et al. Linear energy transfer incorporated spot-scanning proton arc therapy optimization: a feasibility study. Front Oncol. 2021;11:698537.
54. Popescu CC, Beckham WA, Patenaude VV, Olivotto IA, Vlachaki MT. Simultaneous couch and gantry dynamic arc rotation (CG-Darc) in the treatment of breast cancer with accelerated partial breast irradiation (APBI): a feasibility study. J Appl Clin Med Phys. 2013;14:161–75.

Publisher's note